

Coordinated Control of Three-Dimensional Components of Smooth Pursuit to Rotating and Translating Textures

Janick Edinger,¹ Dinesh K. Pai,²⁻⁴ and Miriam Spering^{1,3-5}

¹Ophthalmology & Visual Sciences, University of British Columbia, Vancouver, Canada

²Computer Science, University of British Columbia, Vancouver, Canada

³Institute for Computing, Information and Cognitive Systems, University of British Columbia, Vancouver, Canada

⁴Center for Brain Health, University of British Columbia, Vancouver, Canada

⁵International Collaboration on Repair Discoveries, University of British Columbia, Vancouver, Canada

Correspondence: Miriam Spering, University of British Columbia, Department of Ophthalmology & Visual Sciences, Blusson Spinal Cord Research Centre, 818 W 10th Avenue, Vancouver, BC V5Z 1M9, Canada; mspering@mail.ubc.ca.

Submitted: November 1, 2016

Accepted: January 4, 2017

Citation: Edinger J, Pai DK, Spering M. Coordinated control of three-dimensional components of smooth pursuit to rotating and translating textures. *Invest Ophthalmol Vis Sci*. 2017;58:698–707. DOI:10.1167/iops.16-21038

PURPOSE. The neural control of pursuit eye movements to visual textures that simultaneously translate and rotate has largely been neglected. Here we propose that pursuit of such targets—texture pursuit—is a fully three-dimensional task that utilizes all three degrees of freedom of the eye, including torsion.

METHODS. Head-fixed healthy human adults ($n = 8$) tracked a translating and rotating random dot pattern, shown on a computer monitor, with their eyes. Horizontal, vertical, and torsional eye positions were recorded with a head-mounted eye tracker.

RESULTS. The torsional component of pursuit is a function of the rotation of the texture, aligned with its visual properties. We observed distinct behaviors between those trials in which stimulus rotation was in the same direction as that of a rolling ball (“natural”) in comparison to those with the opposite rotation (“unnatural”): Natural rotation enhanced and unnatural rotation reversed torsional velocity during pursuit, as compared to torsion triggered by a nonrotating random dot pattern. Natural rotation also triggered pursuit with a higher horizontal velocity gain and fewer and smaller corrective saccades. Furthermore, we show that horizontal corrective saccades are synchronized with torsional corrective saccades, indicating temporal coupling of horizontal and torsional saccade control.

CONCLUSIONS. Pursuit eye movements have a torsional component that depends on the visual stimulus. Horizontal and torsional eye movements are separated in the motor periphery. Our findings suggest that translational and rotational motion signals might be coordinated in descending pursuit pathways.

Keywords: smooth pursuit eye movements, rotational motion, torsion, brainstem, saccades

Pursuing moving objects is a fundamental task of the visual system, with significant evolutionary pressures for both predator and prey. Visual pursuit serves to stabilize images of the moving target close to the high-resolution fovea. Pursuit is usually studied in the laboratory using point-like targets. However, natural objects are not point-like and have spatial extent and visible textures; their motion is characterized not only by the translation of a point, but also by rotation of the texture about that point. Therefore ocular “torsion” (the eyes’ rotation about their visual axes) could be useful for pursuit of natural objects.

Ocular torsion is usually considered a consequence of gaze or head position alone, and not of visual stimulus properties. It was well established by the 19th century by Donders’ and Listing’s laws that ocular torsion during fixation depends, in a predictable way, only on the orientation of the eye relative to the head. Previous experimental studies have tested torsion during pursuit, and some acknowledge deviations from Listing’s law during pursuit.¹⁻⁶ However, these deviations were reported to be small, likely due to the use of small targets. Even though torsion can be visually induced by large rotating targets during fixation, known as rotational optokinetic nystagmus,⁷⁻¹⁰ it is unknown if and how torsion is used during pursuit of textures.

Most literature on the brain pathways for smooth pursuit eye movements considers only responses to translational motion.¹¹⁻¹⁶ The brain mechanisms underlying processing of rotational stimulus motion for pursuit have not been studied. On one hand, there is some evidence for separate processing of translational and rotational motion signals driving the optokinetic nystagmus¹⁷ or human perception of translating and rotating visual objects.¹⁸ On the other hand, recent studies have shown coupling of translational and rotational components of optic flow stimuli in brain areas that are also involved with pursuit, such as ventral intraparietal area (VIP).¹⁹

Here we propose that pursuit is a fully three-dimensional task that utilizes all three degrees of freedom of the eye’s rotation, including torsion. We will refer to this as “texture pursuit” and refer to the classical experimental paradigm, utilizing stimuli without significant spatial extent (and hence without detectable rotation), as “point pursuit.” We probed texture pursuit in healthy human subjects by visual stimulation with translating and rotating textures of different sizes and angular velocities while monitoring eye movements in all three dimensions. We provide evidence that the torsional component of texture pursuit is a function of the rotation of the visual texture, aligned with the properties of the visual stimulus, in



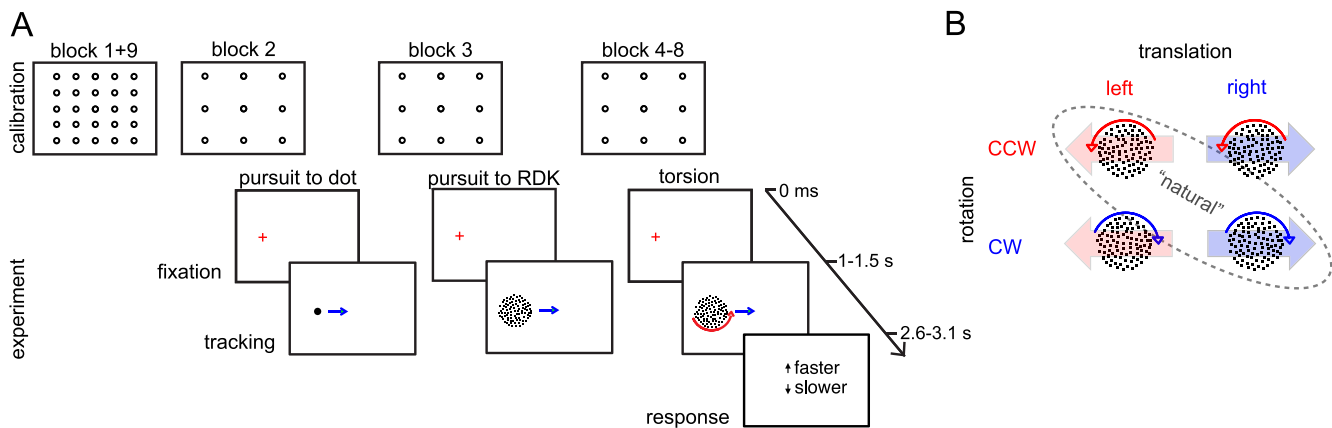


FIGURE 1. Design of experiment 1. (A) Block types and sequence of events in each trial. In blocks 1 and 9, observers made center-out saccades to peripheral locations spaced every 5° in a $25^\circ \times 25^\circ$ grid; these calibration blocks were used to calculate Listing's plane. The experiment consisted of three types of blocks, two pursuit baseline blocks (pursuit to moving dot and nonrotating RDP) and torsion blocks (translating and rotating RDP), all with identical timing and tracking instructions. Each of these blocks (2-8) started with a 9-point calibration. Each trial then began with peripheral fixation followed by stimulus motion; torsion blocks included a judgment of stimulus rotational speed ("faster" or "slower" than the average) via button press. (B) Stimulus rotation conditions in torsion blocks. Leftward stimulus motion and CCW rotation are marked in *red*, rightward motion and CW rotation in *blue*. A combination of right translational motion and clockwise (CW) rotation or left translational motion and counterclockwise (CCW) rotation resulted in a "natural" rotation appearance; the remaining two conditions had an "unnatural" appearance.

violation of Donders' and Listing's laws. By contrast, point pursuit follows Listing's law. Furthermore, we show a tight temporal coupling between corrective saccades in horizontal and torsional directions. Our findings support the view of coordinated processing of translational and rotational motion signals in descending pursuit pathways.

METHODS

In two experiments, we examined the fine spatiotemporal structure of the torsional component of texture pursuit. Head-fixed human observers tracked a translating and rotating random dot pattern while their horizontal, vertical, and torsional eye positions were recorded with a head-mounted eye tracker. Methods apply to both experiments; in experiment 2 we manipulated stimulus size.

Observers

Eight observers (mean age = 26.0, SD = 5.3 years, six female) with normal and uncorrected visual acuity and no history of ophthalmologic, neurologic, or psychiatric disease participated, five observers in each experiment (authors JE and MS participated in both experiments). Experimental procedures followed the tenets of the Declaration of Helsinki and were approved by the University of British Columbia Behavioral Research Ethics Board. All observers participated after giving written informed consent.

Visual Stimuli and Setup

Pursuit stimuli were either small black dots of 0.75° diameter or a random dot pattern (RDP) presented within a disk of 8° diameter (experiment 1) on a uniform white background (55 cd/m^2). The RDP consisted of 400 uniformly distributed black dots (0.05 cd/m^2) that were stationary within the disk, each with a diameter of 0.15° . In a given trial, the textured disk moved across the monitor to the left or right at a constant speed of 10 degrees per second ($^\circ/\text{s}$) for 1600 ms. It either did not rotate (baseline) or rotated around its center in the clockwise (CW) or counterclockwise (CCW) direction at one of five rotational speeds (60, 100, 140, 180, $220^\circ/\text{s}$). These high

rotational stimulus speeds were selected because they are symmetrically distributed around $140^\circ/\text{s}$. This speed was chosen because a disk rolling on a horizontal surface at a horizontal speed of $10^\circ/\text{s}$ without slip would rotate at a speed of $143^\circ/\text{s}$ around its center. The calibration stimulus was a small black dot (a bull's-eye, white inner circle diameter 0.25° , black outer circle diameter 0.75°).

Observers viewed the stimulus in a darkened room on a gamma-corrected 19-inch CRT monitor set to a refresh rate of 85 Hz (ViewSonic Graphic Series G90/B, 1280×1024 , $36.3 \times 27.2 \text{ cm}$; ViewSonic, Brea, CA, USA) with a visible range of 37.8° horizontal \times 28.3° vertical. The viewing distance was 55 cm, and each observer's head was stabilized by a bite bar custom made from dental impression material. Stimulus and procedure were programmed in MATLAB Version R2015b (The MathWorks, Inc., Natick, MA, USA) and Psychtoolbox (Version 3).²⁰

Procedure and Design

We tested observers' eye movements in three different types of blocks. (1) To calculate the location and angle of each observer's individual Listing's plane we conducted two calibration blocks with center-out saccades to peripheral targets at the beginning and end of the experiment (blocks 1 and 9, Fig. 1A). In these blocks, targets were spaced 5° apart on a $25^\circ \times 25^\circ$ grid and presented for 1000 ms following 1500 ms central fixation. Each peripheral location was repeated three times per block, resulting in 75 trials per block. (2) In a pursuit baseline (blocks 2 and 3), we tested pursuit eye movements in response to a moving stimulus that was not rotating, either a single dot (block 2; 32 trials) or a nonrotating RDP (block 3; 32 trials). (3) In experimental blocks 4 to 8 we tested pursuit in response to a translating and rotating RDP.

Each pursuit baseline and experimental block started with a 9-point eye-tracker calibration on targets spaced 10° apart on a $20^\circ \times 20^\circ$ grid. Each trial began with fixation on a red cross (size 1°) at a peripheral location 8° to the left or right of the screen center presented for 950 to 1450 ms (plus a 50-ms blank screen at the end; Fig. 1A). The stimulus then appeared at the location of the fixation cross and moved across the screen for 1600 ms. In experimental blocks, the stimulus had

the appearance of a rolling ball when rightward translational stimulus motion was combined with CW stimulus rotation, or when leftward translational motion was combined with CCW rotation; we refer to this pattern as “natural” and to the opposite pattern as “unnatural” (Fig. 1B). Each observer performed five experimental blocks of 60 trials each, resulting in 300 trials total or 30 trials per condition (5 speed levels \times 2 rotation conditions, natural versus unnatural). At the end of each trial observers judged whether the rotational speed of the stimulus was faster or slower than the average across all previous trials by pressing an assigned key on the computer keyboard. The purpose of this task was primarily to direct observers’ attention to the rotation of the stimulus.

Eye Movement Recordings and Analysis

Eye movements were recorded binocularly with a Chronos ETD (Chronos Vision, Berlin, Germany) at a sampling rate of 200 Hz. This eye tracker is a noninvasive, head-mounted, video-based system that can assess torsional rotations of the eye. It is sufficiently accurate and precise (tracking resolution $< 0.05^\circ$ along all three axes) for the fine spatiotemporal analysis of three-dimensional (3D) eye movements and has been used extensively for this purpose in the literature.^{21,22} We combined this system with a bite bar for head fixation to reduce motion and instability of the head and achieve higher precision in tracking.²³ The 3D eye-in-head position data were processed offline for each eye separately using the Chronos Iris software (Version 1.5) to derive horizontal, vertical, and torsional eye position data from video recordings. The principle of deriving torsional eye position data relies on interframe changes in the iris crypt landmark with each eye rotation. Following standard practice, ocular torsion was obtained from cross-correlation between iris segments across images. Four segments were fitted to each iris (two on each side of the pupil), and angular eye position was calculated as a weighted average from all segments with a cross-correlation factor of >0.7 in that frame. We describe the three components of eye rotation vectors in angular degrees whereby x , y , and z denote horizontal, vertical, and torsional eye rotation, respectively. By convention, leftward, downward, and extorsion (i.e., the top of the eye moving away from the nose) of the right eye and intorsion (the top of the eye moving toward from the nose) of the left eye are positive.

Three-dimensional eye-in-head position data for each eye were processed and analyzed separately using custom-made routines in MATLAB. Eye position data were differentiated to yield eye velocity, and data were filtered with a second-order Butterworth filter (cutoff 15 Hz for position, 30 Hz for velocity). Pursuit onset was detected in a 300-ms interval around stimulus motion onset (starting 100 ms before onset) by fitting each 2D position trace with a piecewise linear function, consisting of two linear segments and one breakpoint. The least-squares fitting error was minimized iteratively (using the function `lsqnonlin` in MATLAB) to identify the best location of the breakpoint, defined as the time of pursuit onset. Catch-up saccades occur naturally during pursuit and were identified using a velocity criterion. Eye velocity had to exceed $20^\circ/\text{s}$ in three consecutive frames to be considered a horizontal or vertical corrective saccade and $10^\circ/\text{s}$ to be considered a torsional corrective saccade. Saccade onsets and offsets were defined as the nearest reversal in the sign of acceleration on either side of the three-frame interval.²⁴ We then computed mean torsional eye velocity in the saccade-free time interval from pursuit onset to stimulus offset, and the number and amplitude of corrective saccades. Horizontal pursuit velocity and velocity gain were computed during steady-state pursuit (interval 200 ms after pursuit onset to stimulus offset) by

dividing horizontal eye velocity by target velocity. We also computed the torsional angle as the total cumulative angle that the eye rotated (extorted or intorted) in the same direction as the stimulus across all saccade-free torsional pursuit segments between pursuit onset and stimulus offset.

That the algorithm correctly identified all aspects of horizontal pursuit and torsion was confirmed by manual inspection of each individual eye trace; traces with blinks, lost signals, or errors in torsion detection were flagged and excluded from further analysis (8.8% across observers, eyes, and experiments). We recorded 3D eye positions from both eyes for each observer. Because the number of usable trials differs between left and right eye for each observer (due to subtle intereye differences in iris shape, structure, and eyelid anatomy), for each observer we selected the eye that yielded a larger number of acceptable trials based on torsion data preprocessing for all analyses.

Listing’s Plane Calibration

Listing’s plane, and the closely related “displacement plane,”²⁵ were estimated from fixation data of calibration blocks 1 and 9 (25 fixation locations) and in the calibration trials at the beginning of blocks 2 to 8 (see Fig. 1A). The Chronos eye tracker reports each eye orientation in Fick coordinates; this was first converted to a 3×3 rotation matrix R , which defines the rotation of an eye-fixed coordinate frame relative to a head-fixed reference frame.²⁶ The rotation matrix was then converted to an axis-angle vector r , defined by the matrix exponential,

$$\exp([r]) = R, \quad (1)$$

where $[r]$ is the 3×3 skew-symmetric matrix representing the cross product with r (i.e., $[r] a = r \times a$, for any vector a). The axis-angle vector is a standard representation of rotations. If we denote the magnitude of the vector as $\|r\| = \theta$, and the unit magnitude vector in the direction of r as \hat{r} , then $r = \theta \hat{r}$; the matrix R corresponds to a rotation by an angle θ about the axis \hat{r} . The axis-angle vector is also known as Euler vector or rotation vector (although, in the oculomotor literature, the term rotation vector is used for the vector $\tan(\theta/2) \hat{r}$, which has the same direction but a different scale factor). Different related vectors have been used in the literature but they define the same Listing’s plane.

Next, the displacement plane for the reference gaze (along the x -axis of the reference frame) was estimated as the best-fitting plane for a set of n axis-angle vectors in the calibration data set. After subtracting the mean, r_0 , of the data set, the vector normal to the plane was estimated using the singular value decomposition (SVD), as the singular vector p corresponding to the smallest singular value of the $3 \times n$ matrix of axis-angle vectors. The offset of the displacement plane from the origin is computed as $p_0 = r_0 \cdot p$, where “ \cdot ” is the dot product of vectors. The plane is completely specified by the three components of $p = (p_1, p_2, p_3)$ and the offset p_0 . The Listing’s plane corresponding to a displacement plane was then computed using the observation of Tweed et al.²⁵ that the displacement plane’s normal vector lies halfway between the gaze vector and the normal to Listing’s plane.

Listing’s Prediction of Ocular Torsion

We computed the torsional velocity predicted by Listing’s law during horizontal pursuit, with speed v , as follows. Since our target always moved along the horizontal axis through the origin, the angular velocity of the eye (a vector, denoted ω)

must lie in the displacement plane (by the “half-angle rule”).²⁷ The vector ω must satisfy

$$p \cdot \omega - p_0 = 0. \quad (2)$$

The velocity vector ω was computed as

$$\omega = \left(- (p_3 v - p_0) / p_1, 0, v \right). \quad (3)$$

It is easy to verify that this ω satisfies the preceding equation and lies in the displacement plane, and hence satisfies Listing's law. The velocity of the visual axis is $\omega \times e_1$, where $e_1 = (1, 0, 0)$ is the reference gaze vector. This velocity moves the eye horizontally with speed v . Finally, the computed angular velocity vector ω was converted to rotational velocity of the eye about each Fick axis at the reference gaze to obtain the predicted torsional velocity.

Statistical Analysis

Effects of stimulus rotational direction (no rotation, CW, CCW) and translational direction (left, right), and further stimulus attributes speed and size were assessed with repeated-measures ANOVAs. All t -tests were paired 2-tailed tests and, if applicable, Bonferroni corrected for multiple comparisons. Statistical analyses were conducted in IBM SPSS Statistics Version 23 (IBM Corp., Armonk, NY, USA).

RESULTS

When tracking a moving and rotating textured visual object with their eyes, human observers generate a pattern of smooth pursuit eye movements that include horizontal and torsional components. Here we show that this texture pursuit scales with visual target properties, and importantly, it differed when tracking natural versus unnatural texture rotation. Figure 2 shows representative eye position traces from one observer's right eye in experiment 1. In baseline trials (RDP without stimulus rotation, Figs. 2A, 2B), the eye smoothly tracked horizontal rightward and leftward stimulus motion (black traces) with occasional horizontal corrective saccades. Baseline torsional rotation (blue traces) produced smooth intorsion or extorsion in alignment with translational stimulus motion direction: CCW for leftward motion and CW for rightward motion (see Fig. 3A, left).

Visual Stimulus Rotation Enhances or Reverses Torsion During Pursuit

This torsional pursuit pattern changed when stimulus rotation was added. Natural stimulus rotation produced torsion in the same direction as in the baseline, that is, CW for rightward motion (Fig. 2C) and CCW for leftward motion (Fig. 2F). As compared to the baseline, however, torsional velocity during natural rotation was enhanced (increased by >50%, see Fig. 3A, right) and rotated across a larger angle (Figs. 2C, 2F). By contrast, unnatural rotation counteracted and reversed torsion from the baseline direction: CCW for rightward and CW for leftward stimulus motion (Figs. 2D, 2E, 3A). Despite individual differences in response magnitude, this pattern of results was consistent across all five observers. Figure 3B shows individual observer torsional velocity relative to the baseline. These data indicate that observed differences in torsional velocity in response to stimulus rotation (CW versus CCW) hold on an individual observer level. Only one data point was close to the diagonal, the line corresponding to no effect of stimulus rotation. Unnatural rotation also triggered more frequent and larger-amplitude torsional corrective saccades as compared to

the baseline (Fig. 3C). Again, this result was consistent across observers (Fig. 3D), with only two data points close to the diagonal. Torsional velocity gain was higher for natural (mean = 0.015, SD = 0.009) than for unnatural rotation (mean = 0.011, SD = 0.007). These results are reflected in significant main effects of rotational direction (CW, CCW, none) on torsional pursuit velocity ($F[2,8] = 45.74$, $P < 0.001$), torsional angle ($F[2,8] = 35.49$, $P < 0.001$), torsional corrective saccade frequency ($F[2,8] = 72.13$, $P < 0.001$), and amplitude ($F[2,8] = 7.43$, $P = 0.02$), as well as significant translational direction (left, right) \times rotational direction interactions for all measures (all $P < 0.01$), signifying differences between natural and unnatural rotation. Main effects of translational direction (left, right) were not significant, indicating left-right symmetry of effects.

In sum, stimulus rotation can either enhance or reverse baseline torsion, that is, either add to or compensate for rotational velocity, depending on whether the rotational direction of the texture is natural or unnatural. Equivalent effects were found in the horizontal component of smooth pursuit (see black traces in Fig. 2): Natural stimulus rotation triggered smooth pursuit with a higher velocity (10% increase in horizontal velocity gain from 0.85 to 0.95; $t[4] = 3.0$, $P = 0.02$) and with a smaller number of horizontal corrective saccades (30% decrease from 2.1 to 1.6 saccades per trial on average; $t[4] = 5.28$, $P = 0.001$) as compared to unnatural rotation. Unnatural rotation also triggered more frequent and higher-amplitude torsional corrective saccades (Fig. 3C), indicating a possible link between both types of corrective saccades.

Synchrony Between Horizontal and Torsional Corrective Saccades

Indeed, Figure 2 indicates that horizontal corrective saccades occurred in synchrony with torsional corrective saccades, fast movements into the opposite direction to torsional pursuit. We analyzed horizontal corrective saccades falling within 50 ms of a torsional corrective saccade (68% of all saccades) and found that horizontal saccades led torsional saccades by only 2.6 ms on average (SD = 9.8). A larger torsional saccade coincided with a larger horizontal eye position change (calculated between torsional saccade onset and offset), indicated by a significant positive correlation (Pearson's $r = 0.59$, $P = 0.01$) between torsional saccade amplitude and concurrent horizontal position change.

Torsion Depends on Visual Stimulus Properties

Torsion also scaled with rotational speed and stimulus size—further indication that torsional pursuit depends on visual features of the stimulus. Figure 4A shows absolute torsional velocity for the five rotational speeds and natural (averaged across right CW and left CCW) versus unnatural (right CCW and left CW) rotational direction. Torsional velocity increased with increasing rotational speed (main effect of speed, $F[4,16] = 10.78$, $P < 0.001$), peaking at 180°/s, then saturated. By contrast, horizontal eye velocity decreased with increasing rotational speed in both natural and unnatural conditions (main effect of speed, $F[4,16] = 15.86$, $P < 0.001$; Fig. 4B).

In experiment 2 ($n = 5$, three of them new observers) we manipulated stimulus size (4°, 8°, 12° diameter, in separate blocks of trials). Differences in stimulus size resulted in different natural rotational speeds: 286°/s for the 4° stimulus, 95°/s for the 12° stimulus translating at a horizontal speed of 10°/s. To enable comparisons across experiments, we kept rotational velocities constant regardless of stimulus size. Torsional velocity increased with stimulus size, as indicated

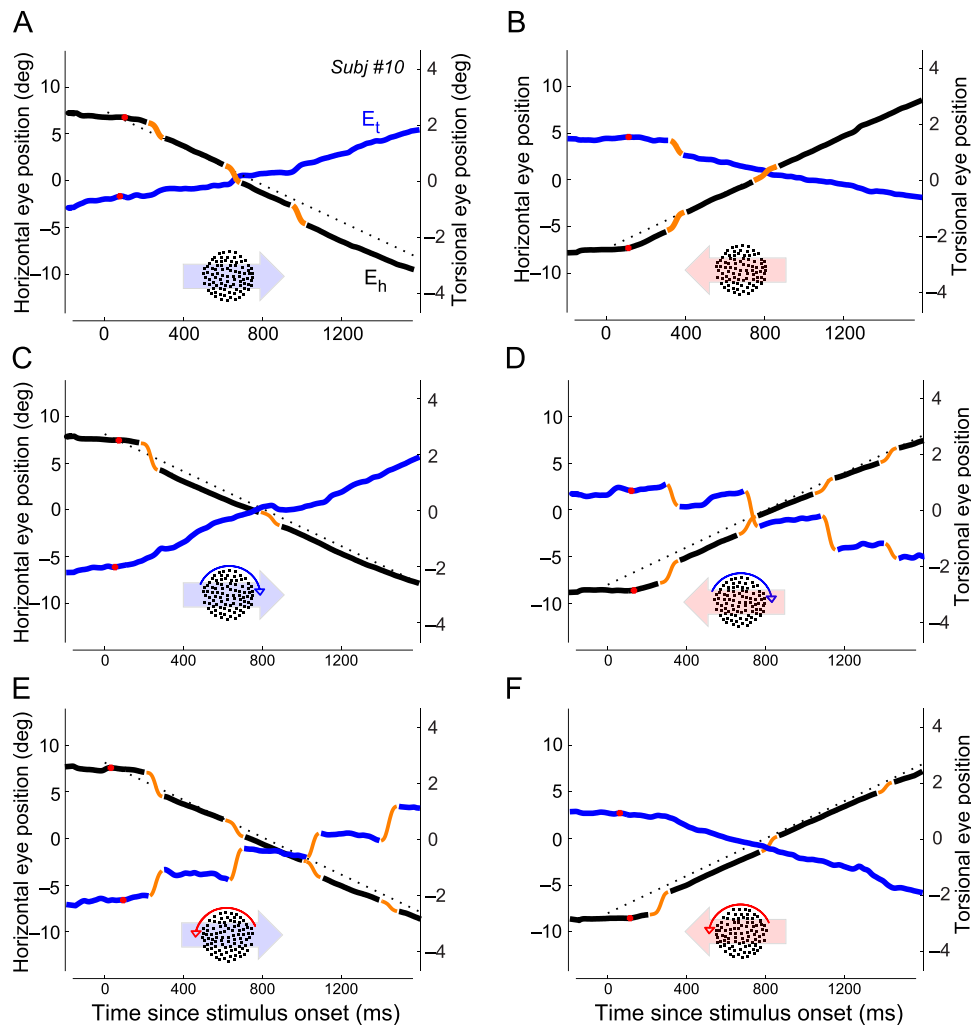


FIGURE 2. Horizontal (*black*; E_h) and torsional eye position (*blue*; E_t) in individual trials from one representative observer in experiment 1. (**A**, **B**) Baseline trials with leftward and rightward motion of a nonrotating RDP. (**C**, **D**) Torsion trials with clockwise rotation. (**E**, **F**) Counterclockwise rotation. Onset of horizontal and torsional tracking component marked in *red*, corrective saccades are indicated in *orange*. *Dotted black line* shows horizontal target position. Torsional position is not shown because high rotational speed of the target renders stimulus position uninformative (see Methods).

by a main effect of size ($F[2,8] = 5.58$, $P = 0.03$; Fig. 4C). This experiment also replicated effects of natural versus unnatural rotation (translational direction \times rotational direction interaction: $F[1,4] = 26.17$, $P = 0.007$; Fig. 4C). As in experiment 1, torsional velocity gain was higher for natural (mean = 0.014, SD = 0.006) than for unnatural rotation (mean = 0.007, SD = 0.005). Horizontal eye velocity tended to decrease with increasing stimulus size (Fig. 4D), but this decrease was nonsignificant ($F[2,8] = 1.5$, $P = 0.28$).

Perception of Rotational Speed

In both experiments, observers were asked to judge the relative rotational speed of the texture at the end of each trial. The main purpose of this task was to ensure that observers attended to the rotational aspect of the stimulus throughout the experiment. Perceptual data in Figure 5 reveal similarities in the perception of natural versus unnatural rotating textures in experiment 1 (no main effect of stimulus condition natural versus unnatural: $F[1,4] = 0.1$, $P = 0.93$; Fig. 5A). The results for experiment 2 suggest a small shift in psychometric data—natural was perceived slightly faster than unnatural for medium rotational speeds (Fig. 5B). However, this small shift was nonsignificant

($F[1,4] = 1.46$, $P = 0.29$), possibly because of the small sample size ($n = 5$). We found no significant interactions between condition (natural versus unnatural) and speed or size.

Listing's and Displacement Planes

To determine alignment of pursuit with Listing's plane, we first analyzed the stability of Listing's plane across all blocks by comparing the estimates of the corresponding displacement plane. The displacement plane was chosen since it is yoked to Listing's plane and it is directly used in predicting torsional eye velocities. For each observer, we computed the angle between the displacement plane for each block and the mean displacement plane across all blocks. The average angular deviation of each block's displacement plane from the mean displacement plane was small (range, 0.8–1.6 across observers, mean = 1.2°), indicating that the displacement and Listing's planes were stable in our experimental setup.

Using the mean displacement plane for each subject, we computed the torsional velocity that would be observed if Listing's law held separately for temporal and nasal directions. For the baseline blocks, Figure 6A shows almost perfect correlations (all $r > 0.80$, $P < 0.05$) between measured

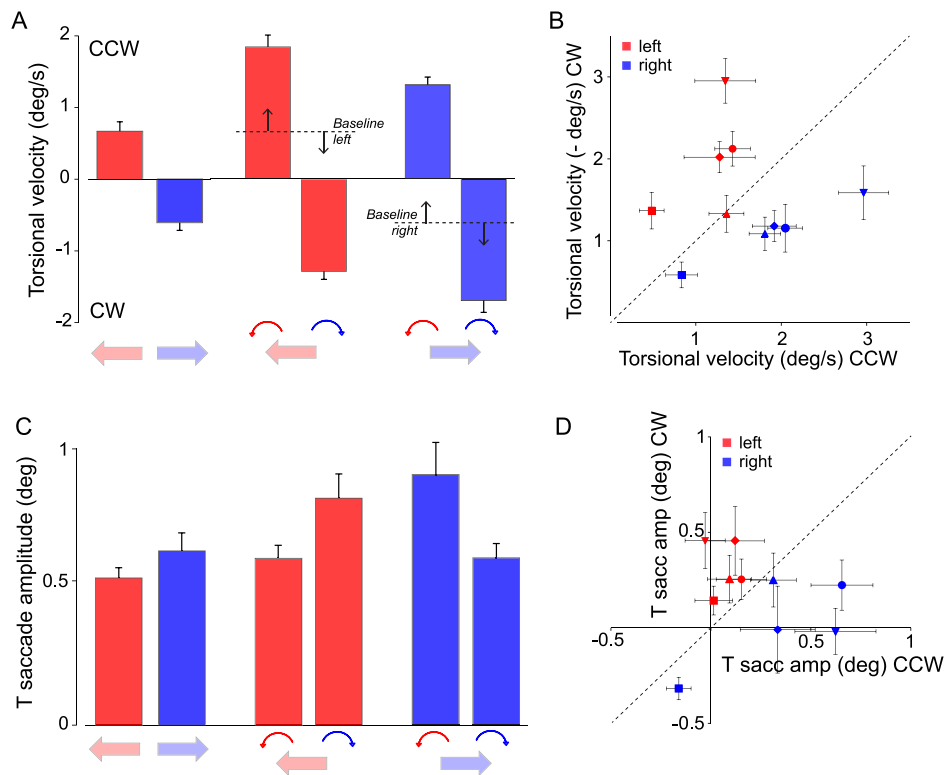


FIGURE 3. (A) Average torsional velocity in baseline blocks (*left*) and in response to natural and unnatural texture rotation (*right*) for five observers. CCW rotation during baseline leftward pursuit and CW rotation during baseline rightward pursuit are in accordance with Listing's law. In torsion blocks, natural motion enhances baseline torsion, unnatural motion reverses baseline torsion. Baseline torsion indicated by *dashed black line*. *Error bars* are standard errors. (B) Individual observer torsional velocity in response to CCW versus CW rotation in leftward (*red*) and rightward pursuit (*blue*) calculated relative to the baseline. Individual observers' mean values are denoted by *symbol type*. For ease of comparison we multiplied the CW torsion value by -1 in the plot. *Error bars* are standard deviations of each individual observer's mean. (C) Torsional corrective saccade amplitude in baseline blocks (*left*) and in response to natural and unnatural motion (*right*). *Error bars* are standard errors. (D) Individual observer torsional saccade amplitude in response to CCW versus CW rotation in leftward (*red*) and rightward pursuit (*blue*). *Error bars* are standard deviations of each individual observer's mean.

torsional velocities (pursuit to dot indicated in gray, pursuit to RDP in black) with predicted torsional velocities based on Listing's law calculations. Torsional velocity during pursuit in the temporal direction (abduction) was closer to the Listing's predictions than in the nasal direction (adduction). Interestingly, pursuit of a dot target (point pursuit) was closer to Listing's prediction than horizontal pursuit of a nonrotating RDP (texture pursuit without stimulus rotation).

Torsional Corrective Saccades Reset the Eye Toward the Displacement Plane

Figure 2 indicates that corrective saccades reset the eye to a torsional equilibrium, from CW to CCW or vice versa, depending on rotational direction (Figs. 2D, 2E). We asked whether these corrective saccades minimize position error, thus correcting to zero torsion, or reset the eye to a fixed location, such as the displacement plane.

We analyzed torsional eye position at the time of saccade onset and offset across all corrective saccades relative to the displacement plane. Eye position distributions from two representative observers are shown in Figures 6B and 6C, revealing a significant decrease in the torsional eye position's standard deviation from the displacement plane at saccade onset (right graph in each case) relative to onset (left graph) in both observers. A repeated-measures ANOVA with factors time (saccade onset versus offset) and rotational direction (natural versus unnatural) yielded a main effect of time ($F[1,4] = 5.54$, P

$= 0.03$), which was stable across directions (no main effect of or interaction with rotational direction, $F < 1$). These findings are congruent with the hypothesis that corrective saccades reset the eye to the displacement plane.

DISCUSSION

Visual rotation has been largely neglected in studies on the visual signals that guide smooth pursuit eye movements,^{16,28,29} and on the brain pathways underlying motion processing for pursuit.¹¹⁻¹⁶ Here we tested pursuit in response to translating and rotating visual stimuli (texture pursuit) and showed that the torsional component of smooth pursuit is aligned with the properties of the visual stimulus. Importantly, torsional pursuit is a function of the rotation of the visual texture, consistent across observers, and thus violates Donders' and Listing's laws positing that ocular torsion depends only on the line of sight. These findings have direct implications for our understanding of natural eye movement behavior when tracking moving objects in our visual environment. By contrast, point pursuit, that is, movements in response to small dots or objects without visual texture or rotation, is mostly consistent with Listing's law, as previously reported.^{3,4,30,31} Pursuit of a dot target (point pursuit) was more closely aligned to Listing's prediction than pursuit of a texture with zero rotational velocity. This suggests that ocular torsion is constrained by

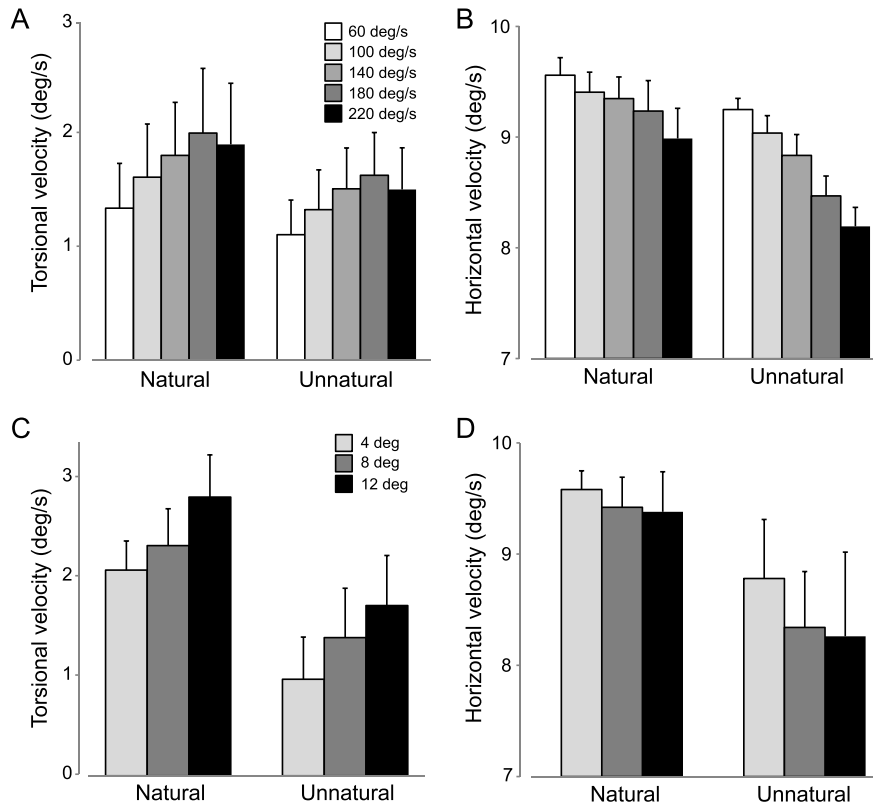


FIGURE 4. Effect of rotational speed on torsional velocity (A) and horizontal pursuit gain (B). Effect of stimulus size on torsional velocity (C) and horizontal pursuit gain (D). All error bars are standard errors of the mean.

the visual stimulus even during pursuit of a purely translating texture. Furthermore, we show a close coordination between horizontal and torsional corrective saccades; these saccades are temporally aligned, and reset the eye to the displacement plane.³²

Neural Mechanisms of Texture Pursuit

Our findings support the view that torsional eye movements are an integral part of pursuit. Visual motion information for the control of smooth pursuit eye movements is extracted in cortical areas MT and MST in mediotemporal and medial superior temporal cortex, respectively.^{13,33,34} Neurons in area MT combine information from primary visual cortex (V1) and

encode the translational direction and speed of moving visual patterns.^{35,36} Rotational motion information is extracted in the dorsal portion of area MST,^{37,38} which contributes to smooth pursuit and analyzes optic flow information for heading.^{11,12,39-43} Thus MST is well positioned to supply information about target rotation that is relayed to brainstem motor nuclei via the dorsolateral pontine nucleus⁴⁴ and the ventral paraflocculus (cerebellar tonsil in humans). Our results suggest that neurons in these motor nuclei may be sensitive to target rotation as well. From the paraflocculus, pursuit-related visual signals reach the separate motor nuclei via the vestibular nucleus and the Y group.⁴⁵

Other descending pursuit pathways may also carry texture pursuit signals, though this has not been investigated. Pursuit

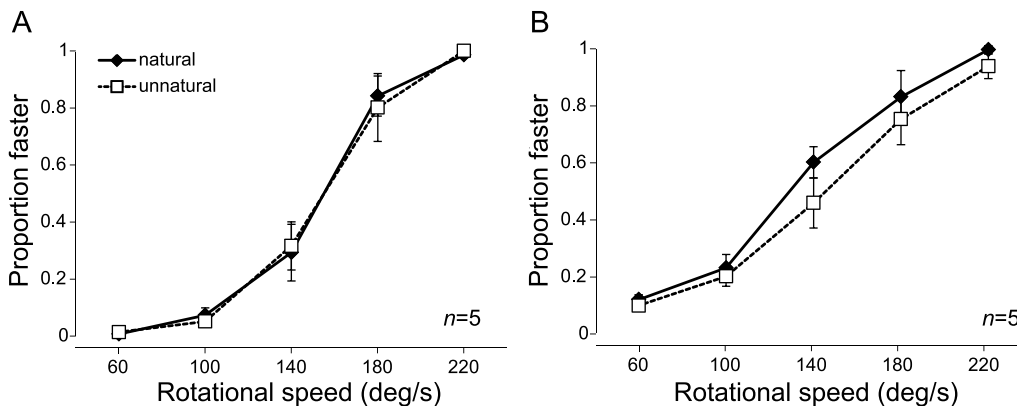


FIGURE 5. Perceptual responses (proportion judgments “faster”) to natural versus unnatural stimulus rotation as a function of rotational speed. (A) Experiment 1. (B) Experiment 2. Error bars denote standard errors of the mean.

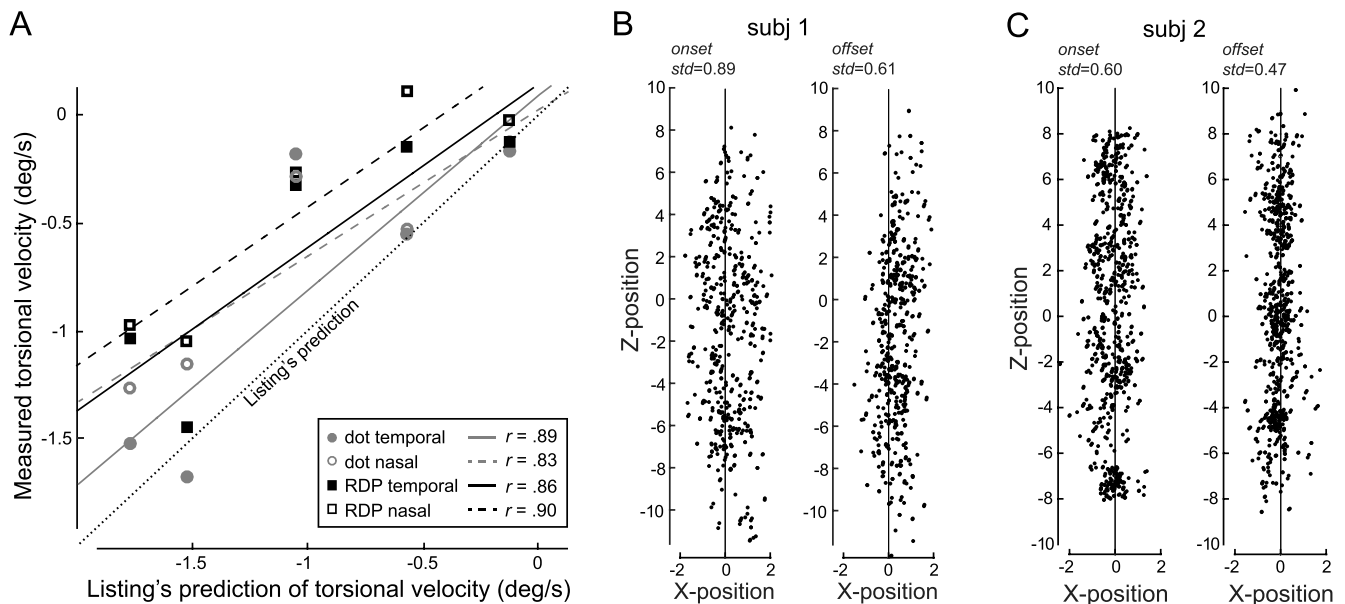


FIGURE 6. (A) Torsional velocity during baseline pursuit to a small dot (gray) or nonrotating pattern (black) is in alignment with torsional velocity predictions based on Listing's plane calculation (dotted diagonal). Each set of the five sets of data points along the vertical is for a single observer in experiment 1 for dot or RDP motion in the temporal (filled symbols) or nasal direction (open symbols). Solid and dashed lines are best fit regression lines; statistics are Pearson's r , all $P < 0.05$. (B) Distributions of torsional eye position at the time of saccade onset (left) and offset (right) across all corrective saccades relative to the displacement plane for subject 1. (C) Torsional eye positions for subject 2. Note that eye positions are in three dimensions; y -axis is perpendicular to the plane of the paper.

signals from the frontal eye fields (FEFsem) reach the motor areas via the nucleus reticularis tegmenti pontis (NRTP) and the cerebellar oculomotor vermis. The caudal NRTP is known to be involved in the stabilization of Listing's plane by correcting torsional eye movements away from Listing's plane during saccades. Neurons in this nucleus thus carry ocular torsion signals during saccades.⁴⁶ Since some MST neurons project to FEFsem,⁴⁷ it is possible that the frontal pursuit pathway also carries ocular torsion signals.⁴⁸ Areas MT and MST also have reciprocal connections with ventral intraparietal area (VIP), a site that contributes to pursuit⁴⁹ and combines translational and rotational components of self-motion.¹⁹

Neural Mechanisms of Torsional Saccades

Our finding of tight temporal coupling between corrective saccades in response to stimulus translation and rotation might have implications for our understanding of saccade control as well. Brainstem saccade control is separate for horizontal and torsional components of saccades.⁵⁰ Any direct coupling between 3D saccade generating systems has been postulated to exist only between torsional and vertical, but not between torsional and horizontal, systems.³² Our findings challenge this view and indicate that there might be cross-coupling between horizontal and torsional signals in descending pathways. We hypothesize that ocular torsion might be an integral part of the common descending input to brainstem motor nuclei, and separate into horizontal and torsional/vertical components only in the motor periphery. However, our study was not designed to specifically address the question how, and at what level of processing, horizontal and torsional saccades might be coupled.

Interestingly, a similar tight coupling exists between saccades and vergence. This assumption is based on the behavioral observation that vergence during horizontal saccades in depth is accelerated. To achieve this facilitation, saccade and vergence commands could be combined (for reviews, see Refs. 51–54).

Texture Pursuit Versus Rotational OKN

Similar to texture pursuit, visually induced rotational optokinetic nystagmus (OKN) and the torsional ocular following response (OFR) also systematically scale with stimulus properties such as rotational speed, stimulus size, location in the visual field, and horizontal disparity.^{7–10,55,56} Even though most of these studies used large rotating textures, horizontal and rotational OFRs can also be elicited by smaller stimuli.^{56–58} Hence, one could argue that observers' texture pursuit in our study might be a superposition of classical (horizontal/2D) point pursuit and rotational OKN/OFR. While such an account can explain effects of stimulus size and speed,⁵⁶ it would predict an additive mechanism, creating symmetric effects of rotational direction (natural versus unnatural rotation) on torsional speed, because CW and CCW rotation produce effects of equal magnitude on torsional OKN.⁸ However, results in Figure 3A show that the addition of stimulus rotation does not simply add to or subtract from baseline torsion by a fixed magnitude. The response to unnatural rotation significantly differs from such a prediction. For example, adding CCW rotation to leftward baseline pursuit (natural) produces an average change of 1.17°/s relative to baseline torsional velocity. Adding CW rotation to leftward pursuit (unnatural) produces a larger change relative to baseline, 1.96°/s on average. The same asymmetry, of similar magnitude, can be observed for adding rotation to rightward pursuit. In line with these findings, unnatural rotation triggers higher-amplitude saccades (Fig. 3B). The eye seems to both add torsional velocity as well as correct for opposite (unnatural) rotation, resulting in a nonlinear effect and producing a pattern of results that differs both quantitatively and qualitatively between natural and unnatural rotation. Furthermore, it is unclear how an additive mechanism, in which the torsional component of texture pursuit is simply rotational OKN or OFR, could account for differences observed between horizontal pursuit to natural versus unnatural rotation (as shown in Fig. 4).

The combination of translational and rotational stimulus motion creates a unique situation in which stimulus motion can be perceived as “natural” or “coherent” versus “unnatural” or “incoherent.”⁵⁹ Our finding shows departure from Listing’s law that depends on such stimulus motion, consistent with the view that pursuit serves to stabilize a relatively small moving target close to the fovea. It is important to note that torsional velocity gain is usually very low, less than 0.1^{8,55,56}; that is, the eye rotates at less than 10% of the rotational target speed. Average torsional velocity gain in our study was 0.013 in experiment 1 and 0.01 in experiment 2. These values are slightly lower than those reported in the literature,^{8,55,56} likely due to the smaller size of stimuli used in our study (4°–12° diameter) and the fact that torsional velocity gain scales with stimulus size (Fig. 4C).⁵⁶

Why Does Unnatural Rotation Cause Slower Horizontal Pursuit?

A previous study examined the kinematics of human horizontal pursuit in response to textures with natural or unnatural rotation, but did not assess the torsional component.⁵⁹ These authors found enhanced horizontal pursuit gain in response to natural rotation and reduced gain when tracking unnatural rotation. They attribute their findings to experience with natural objects and/or the use of internal models of the laws of physics. However, rolling balls are relatively recent developments, and the evolution of the torsional system was likely not substantially shaped by them. While it is well established that experience and internal models guide visual perception and action,^{60,61} our findings provide a much simpler explanation for the rotational tuning of horizontal pursuit gain. During natural rotation, the baseline torsion in the eye movement (produced by pursuing a point), which may be due to Listing’s law, is consistent with the rotational direction of the stimulus, and thus may serve as an agonist to boost the horizontal pursuit response (Fig. 3). By contrast, during unnatural rotation, baseline eye torsion (produced by point pursuit) is opposite to the stimulus rotation and may serve as an antagonist, causing more frequent and larger torsional corrective saccades, thus impairing horizontal pursuit.

It is important to note that rotational stimulus direction did not seem to modulate perceptual performance in our study. Observers processed visual textures in both rotation conditions equally efficiently, with similar sensory gain, regardless of the profound effect of translational and rotational stimulus direction on eye movements. Perceptual results also indicate that visual attention was not a factor contributing to the observed asymmetry in texture pursuit to natural versus unnatural rotation. Despite striking similarities in perceptual performance between natural versus unnatural rotation, the small sample size ($n = 5$) precludes a definitive conclusion regarding perceptual modulation.

Conclusion: Texture Pursuit Is a Three Degree of Freedom Sensorimotor Task

How the oculomotor system utilizes its three rotational degrees of freedom has been a longstanding question in neuroscience. One widely held view is that since the task of positioning the high-resolution fovea on a visual target requires only two degrees of freedom, the oculomotor system has a “redundant” degree of freedom, and that this redundancy is resolved by Listing’s law. Our results show that pursuit has a torsional component that depends on the visual stimulus, providing evidence that pursuit of textured objects uses all three degrees of freedom.

Acknowledgments

Supported by Natural Sciences and Engineering Research Council of Canada Discovery Grants to DKP (RGPIN 153236) and MS (RGPIN 418493), Canada Foundation for Innovation (CFI) John R. Evans Leaders Fund to MS, and CFI Leading Edge Fund to DKP.

Disclosure: **J. Edinger**, None; **D.K. Pai**, None; **M. Sperling**, None

References

- Westheimer G, McKee SP. Failure of Donders’ law during smooth pursuit eye movements. *Vision Res.* 1973;13:2145–2153.
- Ott D, Eckmiller R. Ocular torsion measured by TV- and scanning laser ophthalmoscopy during horizontal pursuit in humans and monkeys. *Invest Ophthalmol Vis Sci.* 1989;30:2512–2520.
- Haslwanter T, Straumann D, Hepp K, Hess BJ, Henn V. Smooth pursuit eye movements obey Listing’s law in the monkey. *Exp Brain Res.* 1991;87:470–472.
- Tweed D, Fetter M, Andreadaki S, Koenig E, Dichgans J. Three-dimensional properties of human pursuit eye movements. *Vision Res.* 1992;32:1225–1238.
- Straumann D, Zee DS, Solomon D, Kramer PD. Validity of Listing’s law during fixations, saccades, smooth pursuit eye movements, and blinks. *Exp Brain Res.* 1996;112:135–146.
- Thurtell MJ, Joshi AC, Walker MF. Three-dimensional kinematics of saccadic and pursuit eye movements in humans: relationship between Donders’ and Listing’s law. *Vision Res.* 2012;60:7–15.
- Howard IP, Templeton WB. Visually-induced eye torsion and tilt adaptation. *Vision Res.* 1964;4:433–437.
- Cheung BSK, Howard IP. Optokinetic torsion: dynamics and relation to circularvection. *Vision Res.* 1991;31:1327–1335.
- Farooq SJ, Proudlock FA, Gottlob I. Torsional optokinetic nystagmus: normal response characteristics. *Br J Ophthalmol.* 2004;88:796–802.
- Ibbotson MR, Price NS, Das VE, Hietanen MA, Mustari MJ. Torsional eye movements during psychophysical testing with rotating patterns. *Exp Brain Res.* 2005;160:264–267.
- Komatsu H, Wurtz RH. Relation of cortical areas MT and MST to pursuit eye movements. I. Localization and visual properties of neurons. *J Neurophysiol.* 1988;60:580–603.
- Komatsu H, Wurtz RH. Relation of cortical areas MT and MST to pursuit eye movements. III. Interaction with full-field visual stimulation. *J Neurophysiol.* 1988;60:621–644.
- Lisberger SG, Movshon JA. Visual motion analysis for pursuit eye movements in area MT of macaque monkeys. *J Neurosci.* 1999;19:2224–2246.
- Ilg UJ. The role of areas MT and MST in coding of visual motion underlying the execution of smooth pursuit. *Vision Res.* 2008;48:2062–2069.
- Mustari MJ, Ono S, Das VE. Signal processing and distribution in cortical-brainstem pathways for smooth pursuit eye movements. *Ann N Y Acad Sci U S A.* 2009;1164:147–154.
- Lisberger SG. Visual guidance of smooth pursuit eye movements. *Annu Rev Vis Sci.* 2015;1:447–468.
- Tian J, Zee DS, Walker MF. Rotational and translational optokinetic nystagmus have different kinematics. *Vision Res.* 2007;47:1003–1010.
- Porter KB, Caplovitz GP, Kohler PJ, Ackerman CM, Tse PU. Rotational and translational motion interact independently with form. *Vision Res.* 2011;51:2478–2487.
- Sunkara A, DeAngelis GC, Angelaki DE. Joint representation of translational and rotational components of optic flow in parietal cortex. *Proc Natl Acad Sci U S A.* 2016;113:5077–5082.

20. Brainard DH. The Psychophysics Toolbox. *Spat Vis.* 1997;10:433-436.
21. Blohm G, Lefèvre P. Visuomotor velocity transformations for smooth pursuit eye movements. *J Neurophysiol.* 2010;104:2103-2115.
22. Murdison TS, Paré-Bingley CA, Blohm G. Evidence for a retinal velocity memory underlying the direction of anticipatory smooth pursuit eye movements. *J Neurophysiol.* 2013;110:732-747.
23. Houben MM, Goumans J, van der Steen J. Recording three-dimensional eye movements: scleral search coils versus video oculography. *Invest Ophthalmol Vis Sci.* 2006;47:179-187.
24. Fooker J, Yeo S-H, Pai DK, Spering M. Eye movement accuracy determines natural interception strategies. *J Vis.* 2016;16(14):1.
25. Tweed D, Cadera W, Vilis T. Computing three-dimensional eye position quaternions and eye velocity from search coil signals. *Vision Res.* 1990;30:97-110.
26. Haslwanter T. Mathematics of three-dimensional eye rotations. *Vision Res.* 1995;35:1727-1739.
27. Tweed D, Vilis T. Implications of rotational kinematics for the oculomotor system in three dimensions. *J Neurophysiol.* 1987;58:832-849.
28. Gegenfurtner KR. The interaction between vision and eye movements. *Perception.* 2016;45:1333-1357.
29. Spering M, Montagnini A. Do we track what we see? Common versus independent processing for motion perception and smooth pursuit eye movements: a review. *Vision Res.* 2011;51:836-852.
30. Ferman L, Collewyn H, Van den Berg AV. A direct test of Listing's law. II. Human ocular torsion measured under dynamic conditions. *Vision Res.* 1987;27:939-951.
31. Tian J, Zee DS, Walker ME. Eye-position dependence of torsional velocity during step-ramp pursuit and transient yaw rotation in humans. *Exp Brain Res.* 2006;171:225-230.
32. Lee C, Zee DS, Straumann D. Saccades from torsional offset positions back to Listing's plane. *J Neurophysiol.* 2000;83:3241-3253.
33. Groh JM, Born RT, Newsome WT. How is a sensory map read out? Effects of microstimulation in visual area MT on saccades and smooth pursuit eye movements. *J Neurosci.* 1997;17:4312-4330.
34. Priebe NJ, Churchland MM, Lisberger SG. Reconstruction of target speed for the guidance of pursuit eye movements. *J Neurosci.* 2001;21:3196-3206.
35. Movshon JA, Adelson EH, Gizzi MH, Newsome WT. The analysis of visual moving patterns. In: Chagas C, Gattass R, Gross C, eds. *Pattern Recognition Mechanisms.* New York: Springer; 1985:117-151.
36. Rust NC, Mante V, Simoncelli EP, Movshon JA. How MT cells analyze the motion of visual patterns. *Nat Neurosci.* 2006;9:1421-1431.
37. Graziano MS, Andersen RA, Snowden RJ. Tuning of MST neurons to spiral motions. *J Neurosci.* 1994;14:54-67.
38. Mineault PJ, Khawaja FA, Butts DA, Pack CC. Hierarchical processing of complex motion along the primate dorsal visual pathway. *Proc Natl Acad Sci U S A.* 2012;109:E972-E980.
39. Page WK, Duffy CJ. MST neuronal responses to heading direction during pursuit eye movements. *J Neurophysiol.* 1999;81:596-610.
40. Fetsch CR, Wang S, Gu Y, DeAngelis GC, Angelaki DE. Spatial reference frames of visual, vestibular, and multimodal heading signals in the dorsal subdivision of the medial superior temporal area. *J Neurosci.* 2007;27:700-712.
41. Bremmer F, Kubischik M, Pekel M, Hoffmann KP, Lappe M. Visual selectivity for heading in monkey area MST. *Exp Brain Res.* 2010;200:51-60.
42. Fujiwara K, Akao T, Kurkin S, Fukushima K. Activity of pursuit-related neurons in medial superior temporal area (MST) during static roll-tilt. *Cereb Cortex.* 2011;21:155-165.
43. Ono S, Mustari MJ. Response properties of MST parafoveal neurons during smooth pursuit adaptation. *J Neurophysiol.* 2016;116:210-217.
44. Mustari MJ, Fuchs AF, Wallman J. Response properties of dorsolateral pontine units during smooth pursuit in the rhesus macaque. *J Neurophysiol.* 1988;60:664-686.
45. Krauzlis RJ. Recasting the smooth pursuit eye movement system. *J Neurophysiol.* 2004;91:591-603.
46. Van Opstal J, Hepp K, Suzuki Y, Henn V. Role of monkey nucleus reticularis tegmenti pontis in the stabilization of Listing's plane. *J Neurosci.* 1996;16:7284-7296.
47. Churchland AK, Lisberger SG. Discharge properties of MST neurons that project to the frontal pursuit area in macaque monkeys. *J Neurophysiol.* 2005;94:1084-1090.
48. Monteon JA, Constantin AG, Wang H, Martinez-Trujillo J, Crawford JD. Electrical stimulation of the frontal eye fields in the head-free macaque evokes kinematically normal 3D gaze shifts. *J Neurophysiol.* 2010;104:3462-3475.
49. Schlack A, Hoffman K-P, Bremmer F. Selectivity of macaque ventral intraparietal area (area VIP) for smooth pursuit eye movements. *J Physiol.* 2003;551.2:551-561.
50. Crawford JD, Cadera W, Vilis T. Generation of torsional and vertical eye position signals by the interstitial nucleus of Cajal. *Science.* 1991;252:1551-1553.
51. Zee DS, Fitzgibbon EJ, Optican LM. Saccade-vergence interactions in humans. *J Neurophysiol.* 1992;68:1624-1641.
52. Cullen KE, Van Horn MR. The neural control of fast vs. slow vergence eye movements. *Eur J Neurosci.* 2011;33:2147-2154.
53. Erkelens CJ. A dual visual-local feedback model of the vergence eye movement system. *J Vis.* 2011;11(10):21.
54. King WM. Binocular coordination of eye movements: Hering's Law of equal innervation or uniocular control? *Eur J Neurosci.* 2011;33:2139-2146.
55. Washio N, Suzuki Y, Sawa M, Ohtsuka K. Gain of human torsional optokinetic nystagmus depends on horizontal disparity. *Invest Ophthalmol Vis Sci.* 2005;46:133-136.
56. Sheliga BM, FitzGibbon EF, Miles FA. The initial torsional Ocular Following Response (tOFR) in humans: a response to the total motion energy in the stimulus? *J Vis.* 2009;9(12):2.
57. Quaia C, Sheliga BM, Fitzgibbon EJ, Optican LM. Ocular following in humans: spatial properties. *J Vis.* 2012;12(4):13.
58. Sheliga BM, Quaia C, Cumming BG, Fitzgibbon EJ. Spatial summation properties of the human ocular following response (OFR): dependence upon the spatial frequency of the stimulus. *Vision Res.* 2012;68:1-13.
59. Souto D, Kerzel D. Like a rolling stone: naturalistic visual kinematics facilitate tracking eye movements. *J Vis.* 2013;13(2):9.
60. Weiss Y, Simoncelli EP, Adelson EH. Motion illusions as optimal percepts. *Nat Neurosci.* 2002;5:598-604.
61. Wolpert DM, Ghahramani Z, Jordan MI. An internal model for sensorimotor integration. *Science.* 1995;269:1880-1882.